Article

JOURNAL OF COMPOSITE MATERIALS

Journal of Composite Materials
2023, Vol. 57(21) 3317–3330

DOI: 10.1177/00219983231184020
journals.sagepub.com/home/jcm
Sage

Extraction and characterization of novel lignocellulosic fibers from *Centaurea hyalolepis* plant as a potential reinforcement for composite materials

Hocine Makri[1,2], Mansour Rokbi[1], Mostefa Meddah[1], Naima Belayachi[3] and Abderraouf Khaldoune[1]

Abstract

The aim of this investigation is to evaluate the use of new lignocellulosic fiber extracted from Centaurea hyalolepis plant as a potential reinforcement for light-weight composite applications. In this study, anatomical structure and morphological surface of Centaurea hyalolepis fiber were conducted. The physical-chemical, thermal, crystalline,mechanical, characteristics of extracted fibers were also examined using Attenuated Total Reflectance-Fourier Transform Infrared (ATR-FTIR), thermogravimetric analysis (TGA), X-ray diffraction (XRD) and tensile test. ATR-FTIR analysis confirmed the existence of the main components of lignocellulosic fiber (lignin, cellulose, and hemicellulose). XRD revealed the presence of cellulose with a crystallinity index of 57.93%.By densimetry, the density of Centaurea hyalolepis was determined as 1.13 g/cm^3. The Centaurea hyalolepis was found to be thermally stable up to 271°C. The kinetic activation energy was determined as 115.943 kJ/mol. Tensile tests revealed that the mean tensile strength and Young's modulus of Centaurea hyalolepis fiber were about 372,5 MPa and 9.036 GPa respectively. Because of the dispersion in the experimental tensile results, the Weibull statistical analysis with two parameters was carried out. Regard these findings, the Centaurea hyalolepis fibers can be a suitable candidate for low density polymeric composites reinforcement.

Keywords

Centaurea hyalolepis, lignocellulosic fibers, stem anatomy, mechanical properties, ATR-FTIR, thermal analysis, X-ray

Introduction

Over the years, the world has become aware of the negative environmental impact resulting from the use of synthetic fibers such as glass, carbon, and Kevlar in polymer composites.[1] This motivated researchers and academics to look for new sustainable and environmentally friendly materials to serve as reinforcements in polymer matrix composites. Natural fibers seem to be the solution, thanks to their inexhaustible natural resources and their multiple properties, especially biodegradability, availability, lightness, renewal, low cost, non-toxicity, good thermal properties, recyclability, and good specific properties.[2] Natural fibers have been receiving more attention and have been successfully applied to a wide range of applications, for instance, furniture, airplanes, automotive, electronic industries, packaging, and construction.[3] Furthermore, because of their low greenhouse gas emissions, good mechanical properties compared to their low density, and low energy requirement for their production, natural fibers have become a potential alternative to synthetic ones, and their use has increased significantly during the last two decades.[4,5,6] With all advantages, there are still some disadvantages,[7] which can be overcome by several surface modifications and methods of treatment to achieve sufficient uses.[3]

[1]Department of Mechanical Engineering, Faculty of Technology, University of M'sila, M'sila, Algeria
[2]LMMS, Laboratory of Materials and Mechanical Structures, University of M'sila, M'sila, Algeria
[3]University of Orléans, INSA CVL, Gabriel Lamé Mechanics Laboratory, Polytech Orléans, 45072, Orléans, France

Corresponding author:
Mansour Rokbi, Department of Mechanical Engineering , University of M'sila, University pole of M'sila, Algeria.
Email: mansour.rokbi@univ-msila.dz

Whatever the source of natural fiber, according to the part of the plant from which the fiber is extracted, such as stems, leaves, seeds, fruit, and roots, there is an enormous amount of variation in the properties of the fiber in terms of chemical composition and physical properties, including thermal stability, mechanical properties, and crystalline properties. This variation can directly affect the quality of the final composite material.[8] Most of the properties of natural fibers depend on their composition as well as on many other parameters, such as the variety, the growth conditions (soil, weather), the growth stage, and the extraction method.[9–15]

In nature, there are a variety of plants that have not yet been identified but that can provide better reinforcement for composite materials. To date, various studies have been carried out on the identification, extraction, and characterization of new cellulosic fibers from different plants, such as *Sansevieria cylindrica*,[16] *Arundo donax L.*,[2] *Trachelospermum jasminoides*,[10] *Cymbopogon flexuosus*,[17] *Silybum marianum*[1] and *Malva sylvestris*[18] for possible use as reinforcing agents in composite applications, due to environmental concerns as well as the increasing industrial requirements on lignocellulosic fibers, research on biodegradable renewable composites reinforced by plant fiber is constantly increasing, and this is in order to obtain the fibers that provide satisfactory mechanical and physical properties. More recently, many researchers' efforts have focused on the extraction and characterization of new vegetal fibers from some Centaurea species. Keskin, et al.[19] have extracted and characterized *Centaurea solstitialis* natural fibers and have reported that the crystallinity index and the density were 71.43% and 1.37 g/cm^3 respectively, the mechanical properties of the fibers are 111.85 ± 24.97 MPa and 3.41 ± 0.62 GPa for the tensile strength and the Young's modulus, respectively. The thermal stability was found to be 273°C.In other hand, Khaldoune et al.,[20] have investigated the properties of a new lignocellulosic fiber extracted from the *Centaurea melitensis* plant. Their study reveals that the crystallinity index is about 47.69% and its density is 1.269 g/cm^3. For the same fiber, the results show that the tensile strength and the Young's modulus values are 336.87 ± 127.53 MPa and 23.87 ± 5.21 GPa, respectively.

The *Centaurea hyalolepis* plant is one of the sources of lignocellulosic fibers, which have not yet been investigated as a possible reinforcement for polymeric materials. The aims of this study are to identify, extract, and characterize the Centaurea hyalolepis fibers in order to assess the potential for their use as reinforcement in composite applications. The morphological, physical, chemical, and mechanical properties were conducted on lignocellulosic fiber extracted from the *Centaurea hyalolepis* plant by using the conventional retting method. The anatomy and the surface morphologies were analyzed using a binocular microscope and scanning electron microscopy (SEM). The thermal properties were determined using thermogravimetric analysis (TGA). The chemical analysis was carried out by Fourier-transform infrared spectroscopy (FTIR), and X-ray diffraction (XRD). Also, the mechanical behavior was carried out using a tensile test and Weibull statistical analysis.

Materials and methods

Materials

Centaurea hyalolepis (CH) is an Algerian species of plants belongs to *Asteraceae* family alternatively composite, commonly known as the sunflower or daisy family.[21] A species that can occur in a Mediterranean climate.[22] The CH plant grows on nitrified soils in hot and dry areas discovered on the edges of roads and fields in the region of M'sila. This plant is a cornflower annual, biennial plant, or herbaceous, perennial, but there are also shrubs, vines, and trees. As *Asteraceae* species, the CH plant has economic importance as food staples, garden plants, and herbal medicines, but outside of their native ranges can be considered weedy or invasive.

Fiber extraction

The CH plant was harvested at maturity. First of all, stems are cleaned to remove dust contaminants using distilled water. After removing leaves and thorns, CH stems are kept immersed in water for 3–4 weeks to allow bio-regeneration and the separation of bark from the stem. CH fibers were isolated from the degraded stems by being washed manually using a water jet, then tied with ropes, dried in open air, and kept in a moisture-proof container; afterwards, CH fibers were oven-dried for 24 h at 60°C to eliminate the moisture. The process of extraction is presented in Figure 1.

Characterization

Anatomy. Only healthy stems are concerned with structural analysis. Before examination, a sample preparation was conducted with a selection of a range of diameters between 6 and 10 mm, followed by histological cuts performed by a manually rotating microtome for cutting plant tissue. Samples of 15–25 µm of thickness were obtained and cut at an adequate length with a sharp knife. The specimens were colored with "carmine green of iodine" in order to allow better identification of the cellulose and lignin. After coloration, the cellulose appears in red and the lignin in green.[18] A microscope equipped with a polarized light unit (Nikon, Japan) was used to realize the histological study. Because of the use of polarized light, the cellulosic tissues appear in red, and the lignified and suberized tissues appear in green.[1]

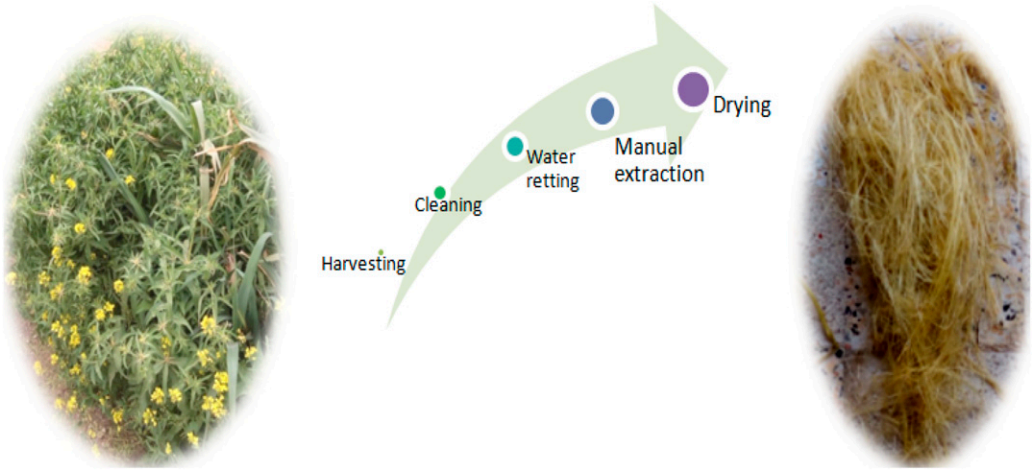

Figure 1. *Centaurea Hyalolepis* extraction process.

Physical properties. To assess the density of the CH fiber, a pycnometer device and Methanol as a liquid of immersion with a density of about 0.792 g/cm^3 at 25°C were used. The weighing process was conducted on an analytical balance with a resolution of 0.00,001 g. Initially, CH fibers were cut into lengths of 15–25 mm. Then, they were dried at 60°C until the moisture content was reduced to below 5%.[23] The relative density was determined using the equation 1:

$$\rho_{CHfibers} = \frac{(W_3 - W_1)}{(W_2 - W_1) - (W_4 - W_3)}\rho_{me} \quad (1)$$

Where ρ_{me} is the density of the liquid in the pycnometer (methanol), W_1 is the mass of the empty pycnometer, W_2 is the mass of the pycnometer filled with methanol, W_3 is the mass of the pycnometer filled with fibers, and W_4 is the mass of the pycnometer filled with fibers and methanol.

The linear density, or more commonly Tex, was obtained from the weight of over 30 single fibers of 200 mm in length each to give a reliable average value. The linear density is calculated by equation 2:

$$D = \frac{M_f}{L} \quad (2)$$

Where D is the linear density or Tex (mg/m), M_f is the mass of fibers (mg), and L is the length of the fiber (m). The cross-sectional area was calculated according to the equation 3.[24]

$$S_f = \frac{M}{\rho_{CH}.L} \quad (3)$$

Where Sf is the fiber cross-section area, M is the fiber mass, L is the fiber length, and ρ_{CH} is the fiber density. Once the density and the linear density were determined, the mean equivalent diameter (De) could be calculated, assuming a cylindrical shape, using the equation 4.[25]

$$De = \sqrt{\frac{4D}{\pi.\rho_{CH}}} \quad (4)$$

X-ray diffraction analysis (XRD). The X-ray diffraction spectra were recorded by the X'Pert-PRO PAN analytical apparatus. The experimental conditions were a monochromatic CuKα X radiation (40kV- 30 mA), a of 0.154 nm, with a scanning speed θ of 2° per minute by a step of 0.050°, the can range 10°–80°. The tests were performed at a lab temperature of 20°C. The Crystallinity Index (CrI) is determined from the height of two peaks, which correspond to the crystalline and amorphous fractions baseline, and was evaluated by using the Segal empirical formula[26,27] as follows

$$C_{rI}(\%) = \frac{I_{002} - I_{am}}{I_{002}}.100 \quad (5)$$

Where I_{002} is the maximum intensity of diffraction of the (002) lattice peak at a 2θ angle of between 22° and 23°, which corresponds to both crystalline and amorphous materials. And I_{am} is the minimum intensity of diffraction of the amorphous fraction, which is taken at a 2θ angle between 16° and 18°, where the intensity is at a minimum. To estimate the crystallite size (CS), Scherrer's equation below was used

$$CS = \frac{K\lambda}{\beta cos\theta} \quad (6)$$

Where K is the Scherrer's constant (K = 0.89), λ is the

spectrum wavelength in A°, β is the whole width of the peak in radians at half maximum, and θ is the diffraction angle.

ATR-FTIR spectral analysis. The Attenuated Total Reflectance Fourier Transform Infrared spectroscopy (ATR-FTIR) technique was used to investigate the chemical composition of CHFs. Fibers were dried for 3 h at 80°C prior to grinding to powder. After that, they were subjected to an ATR-FTIR test. The IR spectra of the CH fibers were recorded using a Perkin Elmer ATR-FTIR with a frequency range of 4000–600 cm^{-1}, at room temperature, operating in ATR mode. Although the ATR mode used is equipped with a module consisting of a diamond crystal of high index, allowing a spectral resolution of 4 cm.

Thermogravimetric analysis (TGA). Thermogravimetric analysis (TGA) measures the amount and rate of change in the weight of CH fibers as a function of temperature or time in a controlled atmosphere. Understanding the thermal decomposition process of fibers allows for better estimation of a composite's behavior during processing. Thermal degradation was conducted on a weighed mass (13 mg) of powdered sample by using a STA449F3 Jupiter apparatus. The spectra were recorded in the range of 43–630°C under an Argon atmosphere (250 mL/min) and at a heating rate of 20°C min^{-1}.

SEM analysis. The surface morphology of longitudinal and transversal sections from the CH plant was characterized by means of a VEGA3 TESCAN scanning electron microscope using an electron beam potential of 20 kV. To avoid electron beam charging effects, the fiber surface was coated with Au-Pd through sputter coating prior to examination.

Tensile tests. CH fibers were manually separated from the bundles and tested according to ASTM D3822-01 standards. Tensile tests were carried out on Zwick/Roell Z100 testing machine equipped with a 5N load cell. Due to the variability of the CH fibers, at least 35 fibers were tested in the as-received state at a gage length of 40 mm in displacement control and at a crosshead speed of 1 mm/min. All tests were performed at an ambient temperature of 25°C and a relative humidity of 28%. More than 30 fibers were tested to determine the average CH fiber properties and standard deviation of fiber and tensile properties (Young's modulus, tensile strength, and strain at failure).

Micro-droplet test. The Micro-droplet test is a method that is used to measure the force capable of causing fiber debonding from the matrix. It can also be used to assess the fiber-matrix adhesion strength as a function of embedding length. In this section, CH fiber composite micro-droplet specimens were used for the fiber Pull-out test. To this end, Micro -drops are made by making knots with epoxy resin around CH fibers. It consists of small drops of epoxy resin applied by a thin metal rod to individual fibers placed in a paper frame and left to harden. Figure 2(b) shows the method of placing the CH fibers on the device and the micro-drop application. The embedded length of the micro -droplet was measured using an optical microscope (MOTIC) equipped with a digital image analyzer (Motic Images Plus 2.0). Figure 2(b) shows the examination of droplet geometry. The force required to debond the solid resin droplet from the fiber while the loading blade held the droplet was recorded. Before testing, the paper frame is cut, and fibers are tested on the Instron ZWICKZ005 universal tensioning test machine for micro-droplet testing on CH fiber. Samples with defects, both in droplets and in fibers, are automatically rejected. Figure 2(c) shows the micro-droplet specimen and test set-up.

The blades are attached to the lower jaw of the Instron test system, and the fibers are pulled through the upper jaw using a head speed of 0.5 mm/min. At least 30 samples were used for Interfacial Shear Strength (IFSS) estimation, and their average value was reported. IFSS that determines the degree of adhesion in a given fibrous matrix system according to the following equation:

$$\tau = \mathrm{IFSS} = F_{max}/\pi dL \quad (7)$$

Where τ is the interfacial shear strength (MPa), F_{max} is the maximum Pull-out force; d is the fiber diameter and L is the embedded length.

Results and discussion

Anatomy

Figure 3 shows observations of transverse sections of *Centaurea hyalolepis* fiber using light microscopy. Reveals the presence of epidermis, chlorenchyma, collenchyma, sclerenchyma, phloem, xylem, and pith, respectively, disposed in layers from the outside to the inside of the cross section of the stem plant.[28] The epidermis, formed by a single cell layer, has as its role the protection of the plant from the external environment, particularly against excessive water loss and invasion by pathogens. The primary phloem tissue is arranged in bundles between the outer cortical tissue and the secondary phloem tissue. Just beneath the cortex, chlorenchyma and collenchyma occurred in alternating segments.[28] Chlorenchyma in red color is composed by the photosynthetic parenchyma cells; it contains abundant, well-developed chloroplasts, and collenchyma in green; their function is primarily mechanical in providing rigidity to the body. Under the collenchyma and the chlorenchyma are the sclerenchyma layers, phloem and xylem, respectively.[10] The sclerenchyma, aggregated in strands, where the fibers were located as bundles, provides a rigid support both in the fundamental and vascular systems

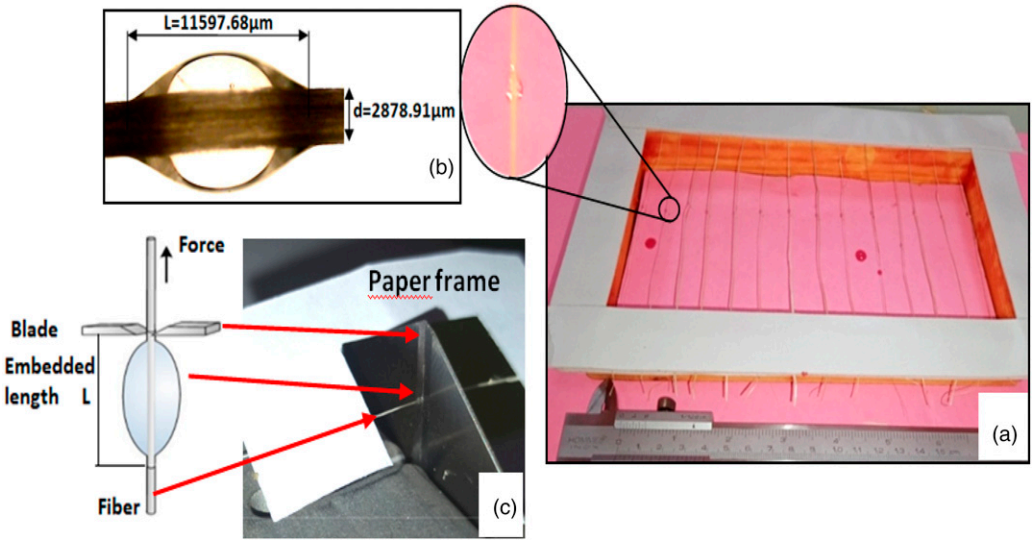

Figure 2. Micro-droplet test procedure: (a) epoxy micro-droplet on individual CM fiber, (b) micro-droplet geometry; (c) micro-droplet specimen and test set-up.

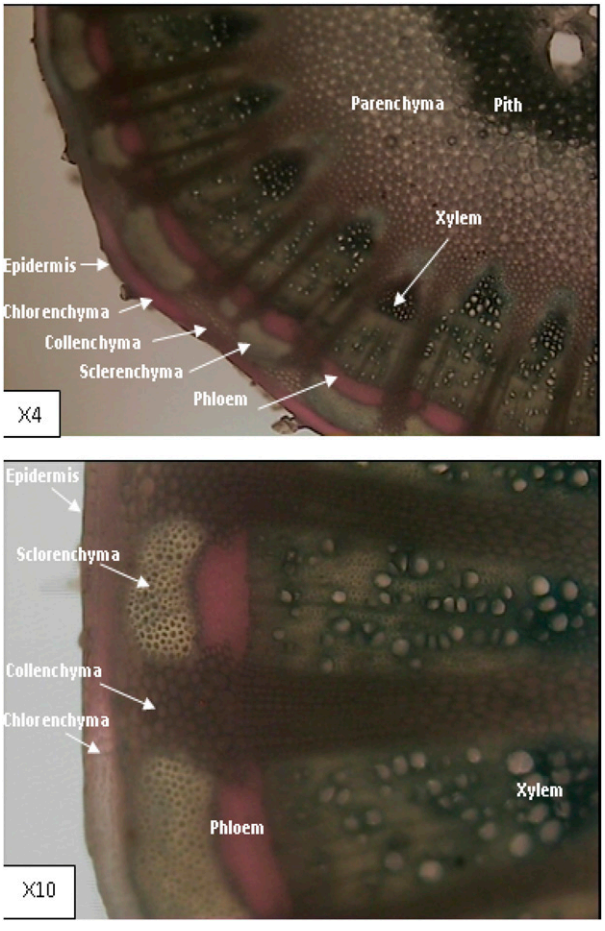

Figure 3. *Centaurea Hyalolepis* stems cross section (x4 and x10 magnifications).

and protects phloem from any damage.[29] The phloem and xylem are grouped in bundles and radially disposed. The xylem on the inner side of the phloem acts as a conducting apparatus for water and inorganic and organic solutes,[29] and also offer mechanical support. The inner part of the plant has pith, which is composed of spongy parenchyma cells that store and transport the nutrients.[10] The diameter of CHFs measured by using an optical microscopereveals diameter ranges from 180 µm to 420 µm.

Density

The density of CH fiber is found to be 1.13 g/cm^3. Comparing this density to others natural fibers densities found in literature provided in table.1. CH density is higher than *Silybum marianum*[1] density but equal to *Malva sylvestris* L[18] and *Juncus effuses* L.[30] However, is lower to comparable fibers of the same species, such as *Centaurea melitensis*[20] and *Centaurea solstitialis.*[19] Although low density is one of the attractive parameters required for the manufacture of lightweight composite materials.

X-ray diffraction analysis (XRD)

The XRD technique was conducted to determine the amorphous and crystalline phases of CH fibers. The XRD patterns obtained are presented in Figure 4. The main crystalline peak characteristic of the cellulose crystallographic plane (200) occurred at 2θ = 22.5° and corresponds to the higher intensity I002 = 285.35. The

Table 1. Comparison of physic properties of different cellulosic fibers from literature.

Fiber	Density (g/cm^3)	Temperature of stability (°C)	Temperature of degradation (°C)	Cristallinity (%)	References
Spartum Lygeum L.	-	220	338.7	46.19	11
Juncus effuses L.	1.139	220	-	33.4	30
Arundo donax	1.168	275	320	-	2
Silybum marianum	1.09	225	357.72	45	1
Malva sylvestris L	1.12	225	485	55.12	18
Centaurea Melitensis	1.26	210	317.86	47.69	20
Centaurea solstitialis	1.37	273	360	71.43	19
Centaurea Hyalolepis	1.13	271	308.9	55.	Current study

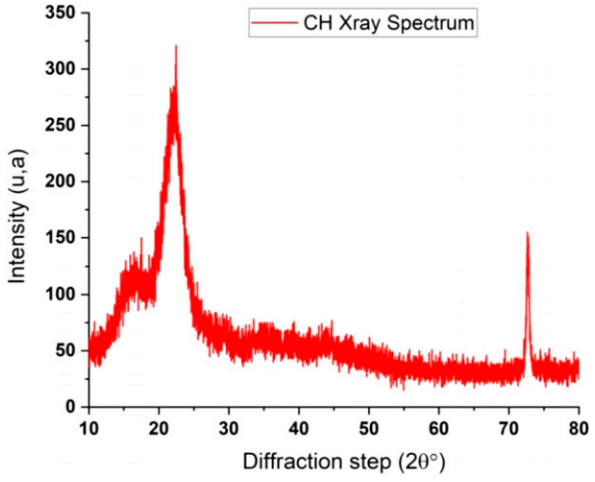

Figure 4. X-ray spectra for CH fibers.

minimum intensity between 002 and 110 peaks (I_{am}) is at 2θ = 16.8°, which specifies amorphous materials (lignin, hemicellulose, pectin, and amorphous cellulose), which corresponds to the lower intensity I_{am} = 126.35. The crystallinity index (CrI) was determined as 55.22% by using equation (5). The average size of a single crystal (CS) is defined by using equation (6) and was estimated at 16.06 nm. The CH fibers have CrI and Cristal Size values comparable to those of *Centaurea melitensis* fibers[20] but are lower than those of *Centaurea solstitialis* fibers.[19] This can be attributed to regularly aligned cellulosic chains. Although higher CrI provides higher tensile properties, and higher thermal degradation temperatures, it also explains why such fibers tend to absorb more water.[31] In comparison with the commonly used based fibers, the crystallinity index of CHFs is lower than that of Jute (71%), Sisal (71%), and Hemp (88%), respectively.[32,33] This may be due to the high amount of non-cellulosic materials.[4]

ATR-FTIR analysis

ATR-FTIR was carried out on untreated CH fibers to analyze the component. The ATR-FTIR spectrum is depicted in Figure 5. The transmittance bands are observed in two wave number regions of 3200–2700 cm^{-1} and 1960–400 cm^{-1}. The identification of the bands is as follows: In the first region, two peaks are identified; a broad peak in the wave number of 3182.89 cm^{-1} is characteristic for stretching vibrations of hydroxyl groups "O-H″ in cellulose molecules.[34,35] A peak located at 2769.16 cm^{-1} is appointed for the asymmetric C-H stretching vibrations of CH and CH_2 in cellulose and hemicellulose.[36,37] In the second zone, several peaks are depicted, the peak appeared in 1456.20 cm^{-1} is associated with the C-H bend in cellulose (the CH_2 and CH_3 deformations bend).[11,36,38] The peaks localized at 1284.75 cm^{-1} are assigned to the C-O stretching vibration of the acetyl group in lignin and hemicellulose, respectively.[1,39,40] The peak depicted in 1183.18 cm^{-1} is associated with C-O-C asymmetrical stretching in cellulose and hemicelluloses[41] and the peak depicted in 1107.70 cm^{-1} is associated with O-H deformation and C-O stretching vibration interaction assigned the group of cellulose and hemicellulose,[1,42] and the peaks appeared in 1021.04 cm^{-1}areassignedto the stretching vibrations of C–O bonding in fibers.[19] The intense peak at 889.65 cm^{-1} is related to the β-glycosidic contribution by cellulose and hemicellulose.[41,43] The functional groups identified in CH fiber are presented in Table 2. The ATR-FTIR spectrum analysis suggests the existence of the main components of natural fiber (lignin, cellulose, and hemicellulose), similar to the most utilized natural fibers such jute,[44] flax,[45] hemp,[33] sisal[46] banana[47] and cotton.[48]

The thermal stability behavior of CH fiber is analyzed by using TGA and DTG curves as represented in Figure 6. The first thermal degradation occurs at 56.97°C with a weight loss of about 9.85%; this could be due to the loss of water

and some moisture in the fibers.[49,50] The second of thermal degradation is identified in the DTG but was not identified on the TGA; it happens at 271°C with a corresponding weight loss of 17.54%. It was found in the literature that such a peak is observed in some natural fibers in the range of 220–300°C. The absence of this peak on TG is probably due to the low amount of hemicellulose in CH fibers.[51,52] The subsequent weight loss associated with the maximum decomposition rate at 308.9°Cwith a weight loss of about 37.32% is assigned to the degradation of cellulose.[52] The last degradation peak is spotted between 360.85°C and 474°C at 386.67°C, with a weight loss of about 25.44% is related to the degradation of the wax and lignin.[53] A residual weight of 9.85% is obtained at up to 600°C. TG/DTG analysis of CH fibers showed that 271°C is the thermal resistance temperature of *Centaurea hyalolepis* fibers. Although, for most natural fibers, approximately 60% of the thermal decomposition occurred within a temperature range between 215°C and 310°C.[54] In accordance with.[19] This temperature is higher than the onset temperature of the most utilized natural fibers, such as Hemp (205.1°C), Kenaf (219°C), Jute (205.1°C).[54] These results suggest that CH fibers can be used as reinforcement in composites if molding of thermoset and thermoplastic polymer matrices occurs under this temperature.

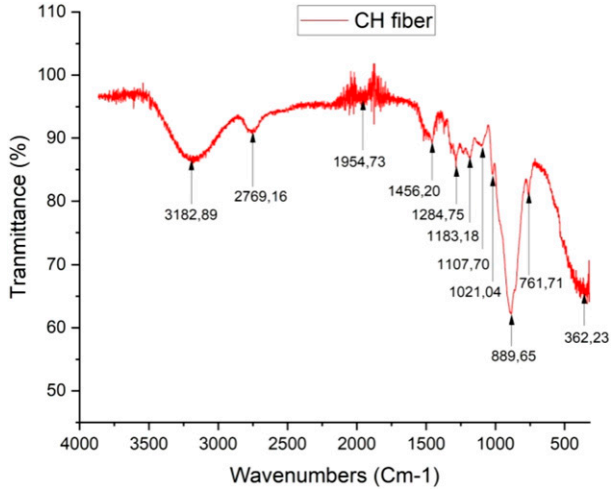

Figure 5. ATR-FTIR spectrum of CH fibers.

The activation energy (Ea), which represents the minimum energy required to initiate fiber degradation, is then the most important kinetic parameter allowing evaluation of the thermal behavior of natural fibers and predicting their thermal decomposition process in order to a subsequent employment as reinforcement in composites. It was calculated for the main fiber degradation step (the decomposition of cellulose) using Broido's method.[55] as follows

$$\ln\left[\ln\frac{1}{y}\right] = -\frac{Ea}{R}\left[\left(\frac{1}{T}\right) + K\right] \quad (8)$$

Where y is the normalized weight (w_t/w_o), wt denotes the weight of the samples at any time t, and wo is the initial weight; Ea is the apparent activation energy; R is the universal gas constant (8.314 kJ/mol); while T is the absolute temperature in Kelvin and K is constant. On the basis of the linear plot of TG shown in Figure 7, the activation energy (E_a) of CH fibers is -115.943 ± 161.56 kJ/mol. The study of the thermal decomposition of CH fibers shows that they can be used as reinforcement in thermoplastic matrix composites.

Table 2. ATR-FTIR bands observed for CH fibers.

Band position For CHFS (cm^{-1})	Wave number range (cm−1)	Origin	Reference
3182.89	3600–3100	O-H hydrogen bond in cellulose	34, 35
2769.16	2950- 2854	CH and CH_2 in cellulose and hemicellulose	36,37
1456.20	1428	CH_2 symmetric bending from cellulose and CH_3 deformations bend	11,36,38
1284.75	1243	C-O stretching vibration of acetyl group in lignin and hemi-cellulose	1,39,40
1183.18	1,170–1,082	C-O-C asymmetrical stretching in cellulose and hemi-celluloses	41
1107.70	1,108	C-H and C-O deformation stretching or bending in lignin	1,42
1021.04	1028	C–O stretching vibrations and bonding	19
889.65	894	β-glycosidic in cellulose and hemi-cellulose	41
761.71	700–900	C-O out-of-plane bending of cellulose	43

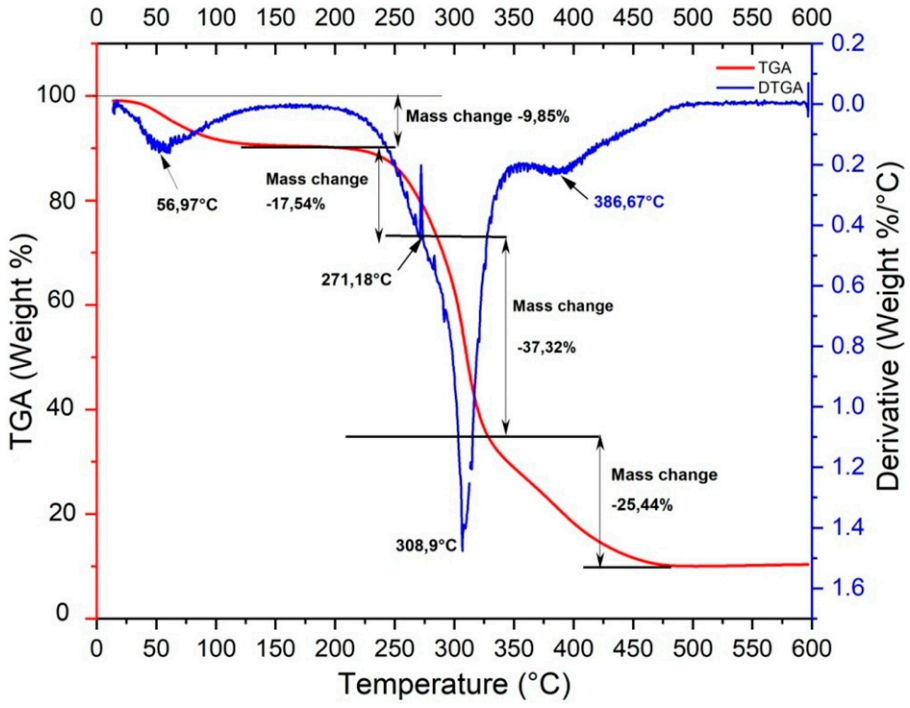

Figure 6. Thermogravimetric curve of CH fiber.

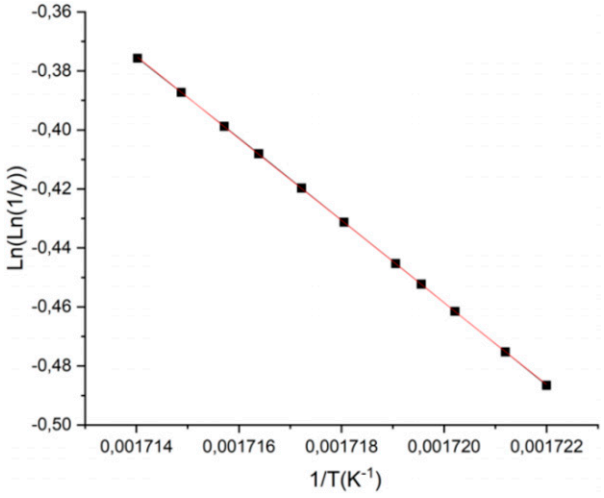

Figure 7. Broido's plot of CH fiber.

Morphological characterizations

SEM analysis was performed on raw CH fibers, and longitudinal and cross-section views are presented in Figure 8. The longitudinal view in Figure (8(a) reveals microfibers covered by non-cellulosic materials so that their surface looks uneven. A few small white particles were observed; they can be wax, lignin, or impurities.[56] By adequate magnification, Figure 8(b) reveals several elementary fibers (or fibrils) bonded together in length direction by pectin, lignin, and other non-cellulosic compounds, forming a bundle.[43,57] The bundle measured 363 μm. Figures (8(b) and (8(c) reveal the rough aspect of the bundle surface because of micro-voids or grooves, fibrils cracks, and impurities such as wax, pectin, lignin, and oil can be observed. However, this roughness is beneficial for the mechanical properties of the composite material because it provides good adhesion to the polymer matrix, while wax and oils provide a protective layer to the fiber surface.[56] The cross-section view in Figure (8(d) shows the fiber-cell structure formed by vascular bundles. The fiber cells were polygonal with a central hole.[28] A variability of the diameters of the fiber cells is noticed; this variability has a great influence on the mechanical properties.

Tensile tests

Tensile testing was employed according to the ASTM D3822-01 Standard to assess the tensile strength, Young's modulus, and strain at failure of CH fibers. A representative stress–strain curve for all tested fibers was shown in Figure 9. It is a typical stress–strain curve, which can be subdivided into two behaviors. First, the stress increases linearly with respect to strain, which corresponds to the linear behavior disturbed by some fluctuations around 0.7% of strain. This behavior could be associated with a global loading of the fiber; through the deformation of each cell wall, the fluctuations can be attributed to rearrangement of the amorphous part of the wall made by pectin and

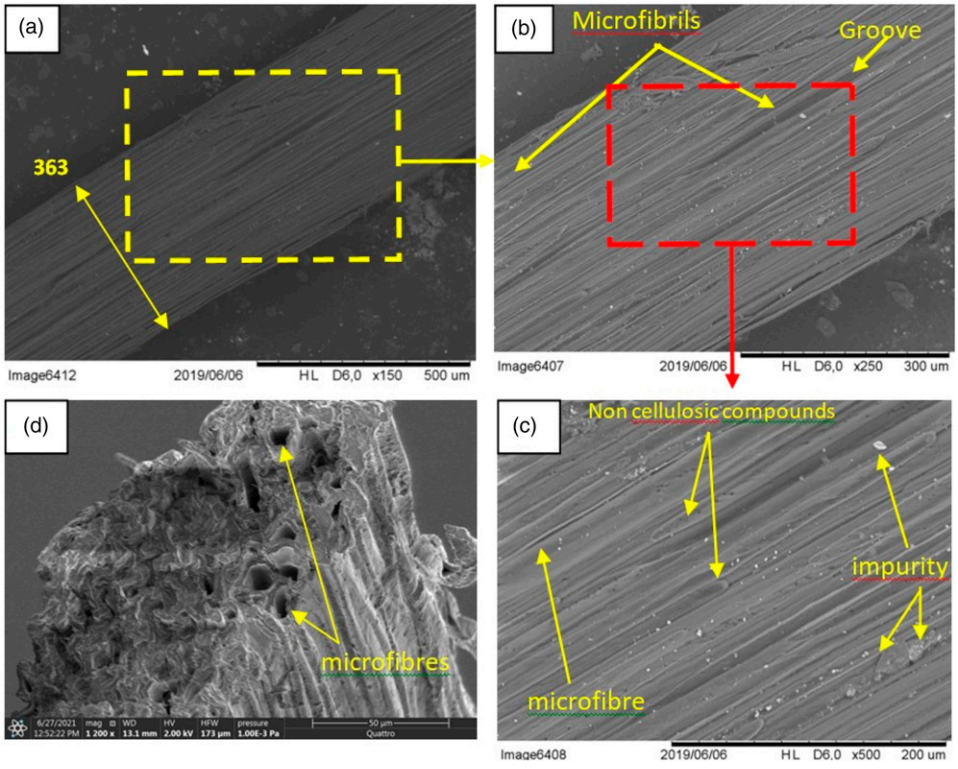

Figure 8. SEM of CH fiber at longitudinal and cross section view at (150x), (250x) and (500x) magnifications.

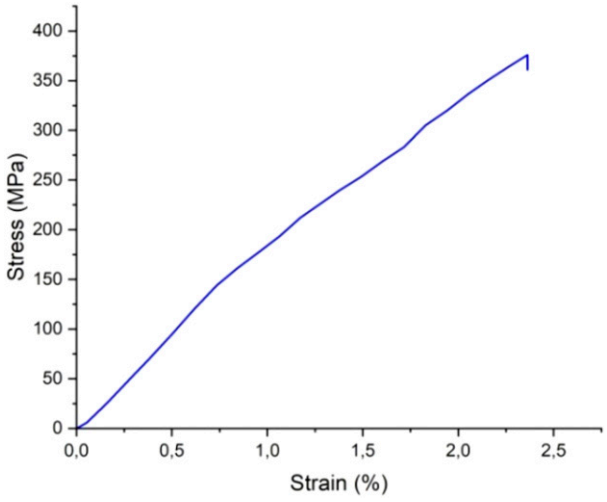

Figure 9. Typical stress–strain curve of CH fiber.

hemicellulose.[2] Second, the load dropped when failure occurred; this behavior corresponds to brittle behavior. Tensile tests revealed that CH fibers have variability in properties. The maximum mechanical strength was in the range of 372.5 ± 2.965 to 191 ± 0.696 MPa, and the strain at break was about 2.36 to 2.02%. The Young's modulus was evaluated through the slope of the curve in the linear region and was in the range of 27.07 ± 3.03 to 11.25 ± 2.28 GPa. This variability in mechanical property values can be attributed to the variation in fiber dimensions. To analyze this behavior, the variation of the tensile strength and Young's modulus versus fiber diameter values were plotted in Figure 10. Given the dispersion of the results, we cannot conclude on the trend of our curves by a simple visual analysis. For this, Origin software been employed to fit the parameter scatter line. This fitting shows a decrease in the tensile strength and the Young's modulus with the fiber diameter. This can be attributed to the fact that the fiber diameters are increased by the rate at which non-cellulosic components such as hemicelluloses, lignin, and pectin providing low strength rather than cellulosic components providing more resistance, and by the weaker or damaged micro-fibrils number. Commonly, the tensile test results of plant fibers are scattered and depend on the age of the plant from which the fiber is extracted, plant properties (source, maturity, plant grown environmental), extraction technique, testing environment. All these factors affect the scattering of results; fortunately there are techniques and programs such as Origin software that help in overcoming difficulties. These results are in agreement with those obtained by other investigators studying natural fibers in this regard.[11,34] Table 3

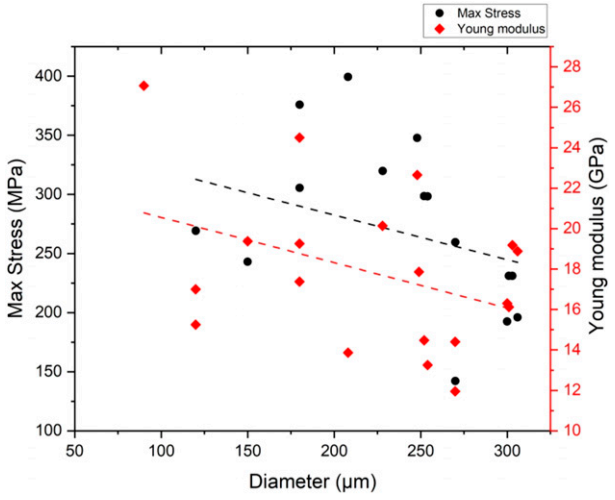

Figure 10. Stress at break and Young's modulus as a function of fiber diameter.

by means of the least squares method, a correlation coefficient of 0.875 is obtained. The average IFSS for fiber-epoxy matrix combinations is 14.24 ± 0.9712 MPa. Although, the interfacial shear strength depends on several factors, some relate to resin property, while others relate to fiber quality, such as roughness, surface area of the fibers and dimensions, which determine the length of the immersed resin for different diameters of fibers and consequently affect the radial stress. The comparison of IFSS shear stress results for CH fibers with other fibers shows that CH fibers/epoxy adhesion strength is greater than *Centaurea melitensis*/epoxy (9.82 ± 2.35 MPa).[20] Basalt/epoxy (11.4 ± 3.1 MPa).[20] IFSS results are Comparable to flax fibers/PLA(poly lactic acid) (14.10 MPa).[38] But still Lower than flax/polyester (18±3 MPa)[58] Hemp fiber/polypropylene (15.4 MPa)[59] and for Abaca fiber/epoxy (31.9 MPa)[60]

Table 3. Comparison of some fiber's mechanical properties.

Fiber	Tensile Strength (MPa)	Young Modulus (GPa)	Elongation at break (%)	References
Juncus effuses L.	113 ± 36	4.38 ± 1.37GPa.	2.75 ± 0.68	30
Spartum Lygeum L	280	13.4	3.7	11
Arundo donax	248	9.4	3.2	2
Silybum marianum	201.16	15.97	1.593	1
Malva sylvestris L	36.64 ± 113	26.07 ± 10.86	1.3 ± 0.6	18
Centaurea Melitensis	336.87 ± 127.53	23.87 ± 5.21	1.27 ± 0.36	20
Centaurea solstitialis	111.85 ± 24.97	3.41 ± 0.62	3.32 ± 0.67	19
Centaurea Hyalolepis	225.11 ± 82.91	17.06 ± 5.56	2.36	Current study

provides a comparison of the mechanical properties of CH fibers with other recent natural fibers in the literature.

Micro-droplet test

In Figure 11, (a) typical force displacement curve is shown. It exhibits some characteristics: the maximum (F_{max}), minimum (F_{min}), as well as the actual embedding length (L). The maximum force applied to the wetted area of the fiber is sufficient for a qualitative estimation of fiber-matrix adhesion strength. After the debonding of the fiber from the matrix, the fiber will be completely pulled out. Thereby, F_{min} is recorded. From the results obtained, the maximum force leading to fiber debonding for the CH fibers is between 6.15 N and 20.68 N.

Based on these measured values and the individual fiber diameters "d", the apparent shear stress "IFSS" can be determined and plotted in Figure 12. Fiber-matrix adhesion strength appeared to depend on embedded length, A linear relationship between debonding load and embedded length is noted. The scatter of data is fairly large. But by line fitting

Weibull statistics

Weibull analysis is the most widely accepted statistical approach that is used to analyze the mechanical properties of cellulosic fibers.[18,61] The common two parameters of the Weibull distribution applied in this study are given by

$$F(\sigma) = 1 - \exp\left(-\frac{L}{L_0}\left(\frac{\sigma}{\sigma_0}\right)^m\right) \quad (9)$$

$$\ln\left(\ln\left(\frac{1}{1-(F(\sigma)}\right)\right) - \ln\left(\frac{L}{L_0}\right) = m(\ln\sigma - \ln\sigma_0) \quad (10)$$

where F (σ) is the failure probability of the fiber, L is the reference length, and L_0 is the initial length σ and σ_0 are respectively defined as the applied stress and characteristic strength and m is the Weibull modulus.

The parameters of the Weibull distribution were calculated through a linear regression analysis using the median rank value estimator, which is defined as follows

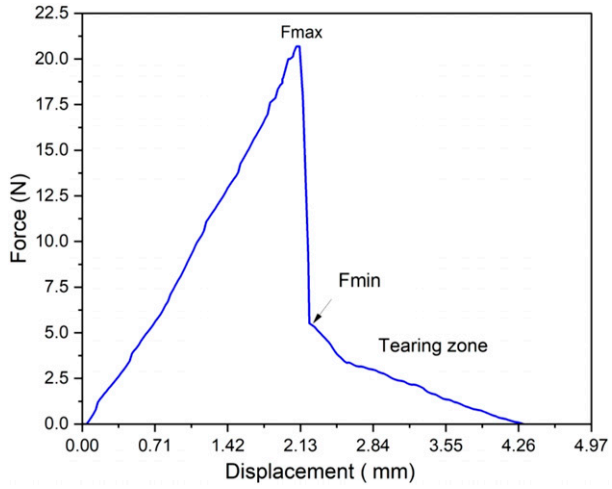

Figure 11. Typical load–displacement diagram of microbond test.

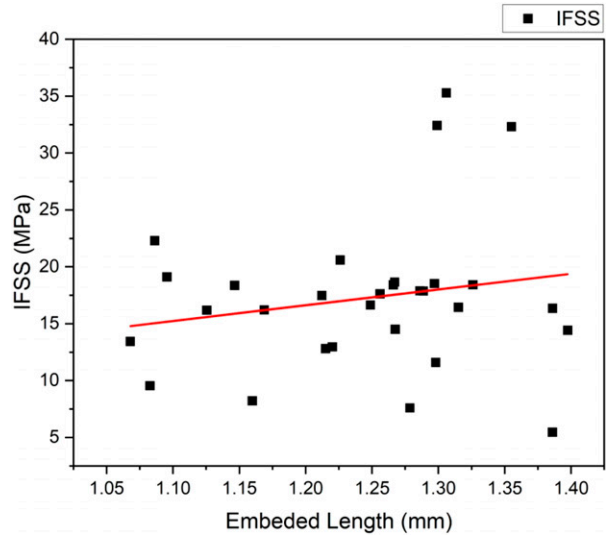

Figure 12. Fiber-matrix adhesion strength in function of embedding length.

$$F(\sigma) = \frac{i - 0.3}{N + 0.4} \quad (11)$$

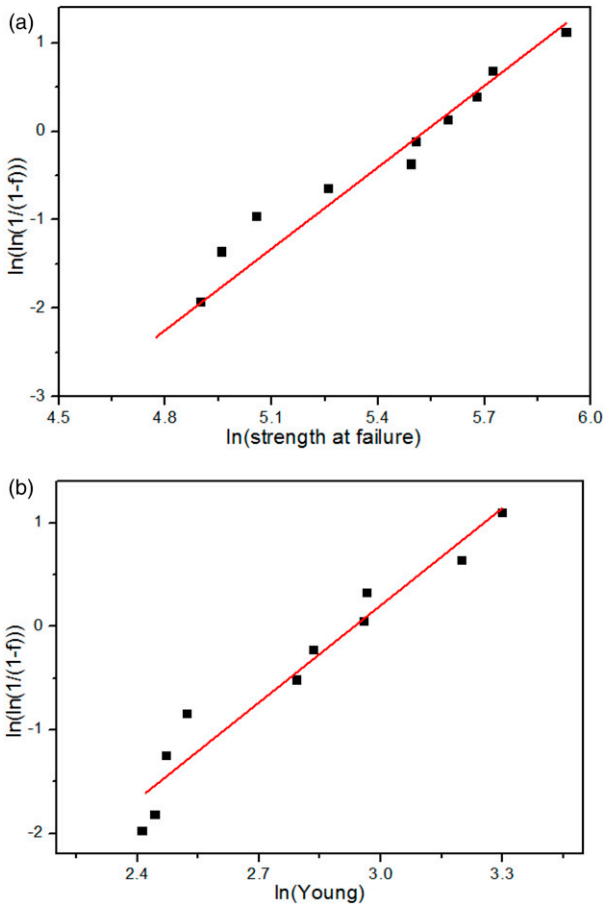

Figure 13. Weibull plot of CH fiber mechanical failure and fitted Weibull reliability distribution for (a) tensile strength and (b) Young's modulus.

Where N is the total number of samples and i is the rank of the i^{th} data point.

Based on equation (10), Weibull plots are shown in Figure 13.

In the case of the most natural fiber, the common values of the Weibull modulus should be confined between 1 and 6.[62,63] In this study, the Weibull modulus found is in the suggested range as indicated in Table 4. On the other hand, Naik and Fronk[61] and Ibrahim, et al.[62] show that the percentage range of error between predicted and measured strengths of Kenaf fiber is approximately 12%. Conversely, in the case of the *Centaurea hyalolepis*

Table 4. Mechanical characteristics of CH fibers obtained by Weibull distribution.

	Tensile strength (MPa)				Young's modulus (GPa)			
	Weibull		exp		Weibull		exp	
Plant species	m	σ_0	σ	Percentage error (%)	m	E_0	E	Percentage error (%)
Centaurea hyalolepis	3.07	252.3a8	225.11	12.11	3.53	19.08	17.06	10.58

fiber study, the same error percentage was found (Table 4). Consequently, the Weibull function is able to characterize the tensile strength and Young modulus of lignocellulosic fibers.

Conclusion

The objective of this study was to characterize new fibers extracted from the *Centaurea hyalolepis* plant in order to assess their properties for potential usability in polymeric composites. The results were discussed, and the following conclusions can be drawn:

- CH fiber reveals diameter ranges from 180 to 420 mm, and the main components of ordinary natural plants are present: epidermis, chlorenchyma, collenchyma, sclerenchyma, phloem, xylem, and pith, which are disposed in layers from the outside to the inside of the cross section.
- The density is found to be 1.13 g/cm^3.The crystallinity of the cellulose content of fibers was determined at 55.22% and the average size of a single crystal at 16.06 nm, which is compatible with thermal analysis. According to thermal analysis, fibers are stable up to 271°C and can be destroyed until 308.9°C. A minimum energy (Ea) of -115.943 ± 161.56 kJ/mol is required to initiate degradation.
- CH fibers are mainly composed of cellulose, hemicellulose, and lignin, which are the main components of other natural fibers, such as jute, flax, hemp, sisal, and cotton.
- SEM of raw CH fibers has shown several elementary fibers (or fibrils) bonded together by pectin, lignin, and other non-cellulosic compounds to form a fiber. The microfibers are covered by non-cellulosic materials such as wax, lignin, or impurities so that their surface looks uneven. The bundles surface presented a rough aspect with micro-voids or grooves, fibrils cracks, and impurities. The structure of the fiber cells is formed by vascular bundles. The fiber cells are polygonal with a central hole.
- The mechanical properties of CH fibers were assessed by the tensile testing method. Variability of values was obtained and was attributed to the variation of bundle dimension. But in general, the results are in agreement with those of other investigators studying natural fibers.
- The Weibull distribution function allows for a good fit with the experimental data of the tensile strength and Young modulus of lignocellulosic fibers.

Consequently, with acceptable thermal behavior, low density and also relatively high tensile strength, *Centaurea hyalolepis* fibers can be candidate suitable candidate for green composites as reinforcement.

Declaration of Conflicting Interests

The author(s) declared no potential conflicts of interest with respect to the research, authorship, and/or publication of this article.

Funding

The author(s) received no financial support for the research, authorship, and/or publication of this article.

ORCID iDs

Hocine Makri https://orcid.org/0000-0003-3776-0022
Rokbi Mansour https://orcid.org/0000-0001-5856-662X

References

1. Laifa F, Rokbi M, Amroune S, et al. Investigation of mechanical, physicochemical, and thermal properties of new fiber from Silybum marianum bark fiber. *Journal of Composite Materials* 2022; 56: 2227–2238.
2. Fiore V, Scalici T and Valenza A. Characterization of a new natural fiber from Arundo donax L. as potential reinforcement of polymer composites. *Carbohydrate Polymers* 2014; 106: 77–83.
3. Karimah A, et al. A comprehensive review on natural fibers: technological and socio-economical aspects. *Polymers* 2021; 13, p. 4280.
4. Lemita N, Deghboudj S, Rokbi M, et al. Characterization and analysis of novel natural cellulosic fiber extracted from Strelitzia reginae plant. *Journal of Composite Materials* 2022; 56: 99–114.
5. Rohit K and Dixit S. A review-future aspect of natural fiber reinforced composite. *Polymers from Renewable Resources* 2016; 7, pp. 43–59.

6. Mansour R, Abdelaziz A and Fatima Zohra A. Characterization of long lignocellulosic fibers extracted from Hyphaene thebaica L. leaves. *Research Journal of Textile and Apparel* 2018; 22: 195–211.
7. Lotfi A, Li H, Dao DV, et al. Natural fiber–reinforced composites: a review on material, manufacturing, and machinability. *Journal of Thermoplastic Composite Materials* 2021; 34: 238–284.
8. Dhakal, Hom Nath, and Zhong Zhang. The use of hemp fibres as reinforcements in composites. In: Omar Faruk, Mohini Sain (eds) Biofiber reinforcements in composite materials. Woodhead Publishing, 2015, pp 86–103.
9. Marrot L, Lefeuvre A, Pontoire B, et al. Analysis of the hemp fiber mechanical properties and their scattering (Fedora 17). *Industrial Crops And Products* 2013; 51: 317–327.
10. Gedik G. Extraction of new natural cellulosic fiber from Trachelospermum jasminoides (star jasmine) and its characterization for textile and composite uses. *Cellulose* 2021; 28: 6899–6915.
11. Belouadah Z, Ati A and Rokbi M. Characterization of new natural cellulosic fiber from Lygeum spartum L. *Carbohydrate polymers* 2015; 134, pp. 429–437.
12. George J, Sreekala M and Thomas S. A review on interface modification and characterization of natural fiber reinforced plastic composites. *Polymer Engineering and Science* 2001; 41: 1471–1485.
13. Maheshwaran M, Hyness NRJ, Senthamaraikannan P, et al. Characterization of natural cellulosic fiber from Epipremnum aureum stem. *Journal of Natural Fibers* 2018; 15: 789–798.
14. Mr S, Siengchin S, Parameswaranpillai J, et al. A comprehensive review of techniques for natural fibers as reinforcement in composites: preparation, processing and characterization. *Carbohydrate Polymers* 2019; 207: 108–121.
15. Rafiqah, A., Abdan, K., Nasir, M. and & Asim M. Effect of extraction on the mechanical physical and biological properties of pineapple leaf fibres. In Jawaid, M., Asim, M., Tahir, P., Nasir, M., (eds) Pineapple Leaf Fibers: Processing, Properties and Applications. Springer, Singapore 2020 pp 41–54.
16. Sreenivasan V, Somasundaram S, Ravindran D, et al. Microstructural, physico-chemical and mechanical characterisation of Sansevieria cylindrica fibres–An exploratory investigation. *Materials and Design* 2011; 32: 453–461.
17. Raja S, Rajesh R, Indran S, et al. Characterization of industrial discarded novel Cymbopogon flexuosus stem fiber: a potential replacement for synthetic fiber. *Journal of Industrial Textiles* 2022; 51: 1207S–1234S.
18. Meddah M, Rokbi M and Zaoui M. Extraction and characterization of novel natural lignocellulosic fibers from Malva sylvestris L. *Journal of Composite Materials* 2022; 57: 897–912.
19. Keskin OY, Dalmis R, Balci Kilic G, et al. Extraction and characterization of cellulosic fiber from Centaurea solstitialis for composites. *Cellulose* 2020; 27, pp. 9963–9974.
20. Raouf Khaldoune A and Rokbi M. Extraction and characterization of novel natural fiber from Centaurea melitensis plant. *Journal of Composite Materials* 2022; 57: 913–928.
21. Ahmad J, Majdi A, Deifalla AF, et al. Concrete reinforced with sisal fibers (SSF): overview of mechanical and physical properties. *Crystals*, 2022; 12, p. 952.
22. Mandel JR, Dikow RB, Siniscalchi CM, et al. A fully resolved backbone phylogeny reveals numerous dispersals and explosive diversifications throughout the history of Asteraceae. *Proceedings of the National Academy of Sciences* 2019; 116: 14083–14088.
23. Amel BA, Paridah MT, Sudin R, et al. Effect of fiber extraction methods on some properties of kenaf bast fiber. *Industrial Crops And Products* 2013; 46: 117–123.
24. Brahim SB and Cheikh RB. Influence of fibre orientation and volume fraction on the tensile properties of unidirectional Alfa-polyester composite. *Composites Science And Technology* 2007; 67: 140–147.
25. Msahli S, Ydrean J and Sakli F. Evaluating the fineness of Agave americana L. fibers. *Textile Research Journal*, 2005; 75, pp. 540–543.
26. Segal L, Creely JJ, Martin A Jr., et al. An empirical method for estimating the degree of crystallinity of native cellulose using the X-ray diffractometer. *Textile Research Journal*, 1959; 29, pp. 786–794.
27. French AD and Santiago Cintrón M. Cellulose polymorphy, crystallite size, and the segal crystallinity index. *Cellulose*, 2013; 20, pp. 583–588.
28. Taşar N, Doğan G, Kiran Y, et al. Morphological, anatomical and cytological investigations on three taxa of Centaurea L.(Asteraceae) from Turkey. *Bangladesh Journal of Plant Taxonomy* 2018; 25: 215–226.
29. KılınÇ AÇ, Köktaş S, Atagür M, et al. Effect of extraction methods on the properties of althea officinalis L. fibers. *Journal of Natural Fibers* 2018; 15: 325–336.
30. Maache M, Bezazi A, Amroune S, et al. Characterization of a novel natural cellulosic fiber from Juncus effusus L. *Carbohydrate Polymers* 2017; 171, pp. 163–172.
31. Indran S, Raj RE and Sreenivasan V. Characterization of new natural cellulosic fiber from Cissus quadrangularis root. *Carbohydrate Polymers* 2014; 110: 423–429.
32. Mwaikambo LY and Ansell MP. Chemical modification of hemp, sisal, jute, and kapok fibers by alkalization. *Journal of Applied Polymer Science* 2002; 84: 2222–2234.
33. Dai D and Fan M. Characteristic and performance of elementary hemp fibre. *Materials Sciences And Applications* 2010; 1: 336–342.
34. Bezazi A, Belaadi A, Bourchak M, et al. Novel extraction techniques, chemical and mechanical characterisation of Agave americana L. natural fibres. *Composites Part B: Engineering* 2014; 66: 194–203.
35. Coates J. *Encyclopedia of analytical chemistry: applications, theory and instrumentation*. Newtown, USA: Interpretation of Infrared Spectra A Practical Approach, 2006.

36. Porras A, Maranon A and Ashcroft I. Characterization of a novel natural cellulose fabric from Manicaria saccifera palm as possible reinforcement of composite materials. *Composites Part B: Engineering* 2015; 74: 66–73.
37. Paiva M, Ammar I, Campos A, et al. Alfa fibres: mechanical, morphological and interfacial characterization. *Composites Science And Technology* 2007; 67: 1132–1138.
38. Kılınç AÇ, Köktaş S, Seki Y, et al. Extraction and investigation of lightweight and porous natural fiber from Conium maculatum as a potential reinforcement for composite materials in transportation. *Composites Part B: Engineering* 2018; 140: 1–8.
39. Seki Y, Seki Y, Sarikanat M, et al. Evaluation of linden fibre as a potential reinforcement material for polymer composites. *Journal of Industrial Textiles* 2016; 45: 1221–1238.
40. Murali Mohan Rao K, Mohana Rao K and Ratna Prasad A. Fabrication and testing of natural fibre composites: vakka, sisal, bamboo and banana. *Materials and Design* 2010; 31: 508–513.
41. Seki Y, Sarikanat M, Sever K, et al. Extraction and properties of Ferula communis (chakshir) fibers as novel reinforcement for composites materials. *Composites Part B: Engineering* 2013; 44: 517–523.
42. Kempaiah R, et al. Ftir and waxs studies on six vegetal fibers. *Interactions* 2020; 12, pp. 19–22.
43. De Rosa IM, Kenny JM, Puglia D, et al. Morphological, thermal and mechanical characterization of okra (Abelmoschus esculentus) fibres as potential reinforcement in polymer composites. *Composites Science And Technology* 2010; 70: 116–122.
44. Ovalı S and Sancak E. Investigation of mechanical properties of jute fiber reinforced low density polyethylene composites. *Journal of Natural Fibers* 2020; 19: 3109–3126.
45. Cao Y, Chan F, Chui Y-H, et al. Characterization of flax fibres modified by alkaline, enzyme, and steam-heat treatments. *BioResources* 2012; 7, pp. 4109–4121.
46. AGGerezgiher H and Asimon T. *Development and characterization of sisal fiber reinforced polypropylene composite materials 4.1*: International Journal of Engineering and Management Sciences 2019; 348–358.
47. Bekraoui N, El Qoubaa Z, Chouiyakh H, et al. Banana fiber extraction and surface characterization of hybrid banana reinforced composite. *Journal of Natural Fibers* 2022; 19: 12982–12995.
48. Bajpai S. K, G. Mary and N. Chand. The use of cotton fibers as reinforcements in composites. In Omar Faruk and Mohini Sain (eds) Biofiber reinforcements in composite materials. Woodhead Publishin 2015, pp. 320–341.
49. Portella EH, Romanzini D, Angrizani CC, et al. Influence of stacking sequence on the mechanical and dynamic mechanical properties of cotton/glass fiber reinforced polyester composites. *Materials Research* 2016; 19: 542–547.
50. Ridzuan M, Abdul Majid M, Afendi M, et al. Characterisation of natural cellulosic fibre from Pennisetum purpureum stem as potential reinforcement of polymer composites. *Materials and Design* 2016; 89: 839–847.
51. Baskaran P, Kathiresan M, Senthamaraikannan P, et al. Characterization of new natural cellulosic fiber from the bark of dichrostachys cinerea. *Journal of Natural Fibers* 2018; 15: 62–68.
52. Saravanakumar S, Kumaravel A, Nagarajan T, et al. Characterization of a novel natural cellulosic fiber from Prosopis juliflora bark. *Carbohydrate polymers* 2013; 92, pp. 1928–1933.
53. Yang H, Yan R, Chen H, et al. Characteristics of hemicellulose, cellulose and lignin pyrolysis. *Fuel* 2007; 86, pp. 1781–1788.
54. Yao F, Wu Q, Lei Y, et al. Thermal decomposition kinetics of natural fibers: activation energy with dynamic thermogravimetric analysis. *Polymer Degradation And Stability* 2008; 93: 90–98.
55. Broido A. A simple, sensitive graphical method of treating thermogravimetric analysis data. *Journal of Polymer Science Part A-2: Polymer Physics* 1969; 7: 1761–1773.
56. Senthamaraikannan P and Kathiresan M. Characterization of raw and alkali treated new natural cellulosic fiber from Coccinia grandis.L. *Carbohydrate Polymers* 2018; 186: 332–343.
57. Fiore V, Valenza A and Di Bella G. Artichoke (Cynara cardunculus L.) fibres as potential reinforcement of composite structures. *Composites Science And Technology* 2011; 71: 1138–1144.
58. Joffe R, Andersons J and Wallström L. Strength and adhesion characteristics of elementary flax fibres with different surface treatments. *Composites Part A: Applied Science And Manufacturing* 2003; 34: 603–612.
59. Beckermann G and Pickering K. Engineering and evaluation of hemp fibre reinforced polypropylene composites: micromechanics and strength prediction modelling. *Composites Part A: Applied Science And Manufacturing* 2009; 40: 210–217.
60. Cai M, Zou Z, Nakagaito AN, et al. Effect of aerobic exercise on blood lipid and glucose in obese or overweight adults: a meta-analysis of randomised controlled trials. *Composites Part A: Applied Science And Manufacturing* 2016; 10: 589–602.
61. Naik DL and Fronk TH. Weibull distribution analysis of the tensile strength of the kenaf bast fiber. *Fibers And Polymers* 2016; 17: 1696–1701.
62. Ibrahim, I., Sarip, S., Bani, N., Ibrahim, M. & Hassan, M. The Weibull probabilities analysis on the single kenaf fiber. in AIP Conference Proceedings (eds Henk Metselaar, Wong Yew Hoong, Reza Mahmoodian & Mohd Fadzil Jamaludin) Kuala Lumpur, Malaysia, 24–25 October 2017, paper no. 1958, 020009, pp.1–7, AIP Publishing LLC, 2018.
63. Wang F and Shao J. Modified Weibull distribution for analyzing the tensile strength of bamboo fibers. *Polymers* 2014; 6, pp. 3005–3018.